Pol. J. Environ. Stud. Vol. 32, No. 1 (2023), 509-517
DOI: *10.15244/pjoes/155149* ONLINE PUBLICATION DATE: 2022-12-22

Review

Research on the Permeability of Water and Sand in the Fractured Rock

Yu Liu[1,3], Wei Li[1], Shuncai Li[1,3]*, Liqiang Ma[2]

[1]School of Mechatronic Engineering, Jiangsu Normal University, Jiangsu, China
[2]School of Mines, China University of Mining and Technology, Jiangsu, China
[3]State Key Laboratory of Coal Resources and Safety Mining, China University of Mining and Technology, Jiangsu, China

Received: 16 July 2022
Accepted: 4 October 2022

Abstract

The water and sand inrush is very factor to influence the safety production of mining. In order to understand the mechanism of water and sand flow in the fracture, the seepage system was designed and manufactured to test the permeability of water and sand in the fractured rock. According to the seepage test, the magnitude of the effective fluidity was in 10^{-8}~$10^{-5}m^{n+2}$. S^{2-n}/kg, while non-Darcy factor β ranged from 10^5 to 10^8 m^{-1}. The relationship of the effective fluidity and non-Darcy factor β- (Joint Roughness Coefficient) JRC was fitted using the exponential function. The equations of effective fluidity and non-Darcy factor were obtained by using the genetic algorithm and the fitting parameters were obtained. The main and secondary factors that affect the permeability include the fracture aperture, roughness, concentration and particle size. Through simulation, it was found that the roughness exhibited no significant effect on the pressure field; however, it did have a significant effect on the velocity field. Velocity of water and sand keeps 1.62 m/s, which increases prominently with the *JRC* increase. The safety regions are deduced under different coefficient *n*. The study is important to explore the mechanism of water and sand inrush.

Keywords: fracture, water-sand, non-Darcy seepage, roughness

Introduction

The amount of coal occupied by northwest China accounts for 80% of the total coal reserves, where the resources are buried shallowly and the method of rapid advance is often adopted. This mining method leads to sliding instability of the stress block beam and the failure of overburden strata, which induces a connected fracture [1]. Along with the movement of the surface water or groundwater, the sand layer flows to mine goaf through the fractured rock, which often leads to the disaster of water inrush and sand collapse, as shown in Fig. 1 [2]. During mining, it will influence the movement and quantity of groundwater [3-4]. Water-sand flow and rock fracture during mining consist of coupling system, which is difficult to study [5].

From the perspective of the seepage loss stability, water inrush and sand collapse are that motion of fluid or solid loses stability, in which the aperture and roughness is important factors that exert considerable effects on the deformability, strength, and permeability characteristics [6-9]. Earlier reports present the effects

*e-mail: zsclsc@263.net

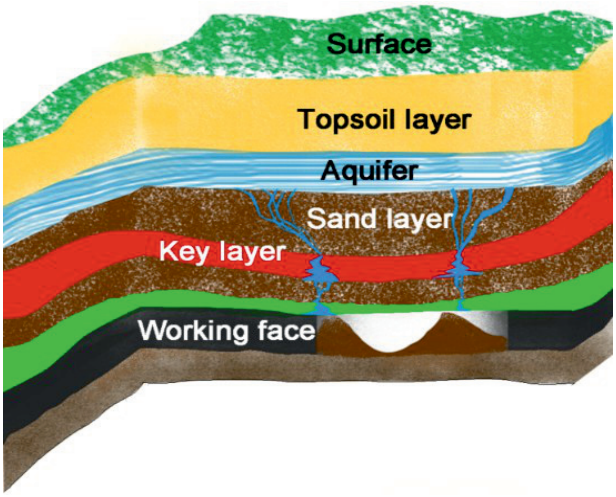

Fig. 1. Water and sand inrush.

of the fracture angle, aperture, fracture network, and fracture roughness [10, 11] influence on the permeability. Also, the effects of fluid like acid [12], two-phase flow [13], heat [14], and sometimes stress and shear stress [15, 16] were considered, in which the problem of permeability became more complicated. Thus, literature reveals that the roughness has an important influence on permeability, both experimental and numerical simulation methods.

Roughness of fracture is a very important factor governing the permeability. Hence, the characteristics and impression of the roughness need to be comprehensively analyzed. The anisotropy of fracture roughness is always related to the height, shape, dip angle, size, arrangement, density and overall fluctuation of the fracture surface [17, 18]. After precise approaches were developed to express the roughness, typical description of roughness in the field was reported [19].

Realistic rock fracture is a complex interior geometrical structure, including infilling materials and contact areas. A full consideration of these interior properties can ease the difficulties in conducting studies on the rock fractures. Therefore, it is necessary to form essential simplifications and assumptions. Based on the aforementioned characteristics of the fracture geometries, many measurement techniques and characterization methods were proposed to quantify the fracture roughness. The measurement techniques of roughness are generally divided into contact and non-contact techniques [20, 21]. JRC was proposed by Barton [22], while many mathematical formulas were deduced by some scholars [23-25]. The fractal theory is considered as an effective tool to quantify the irregular geometries and structures [26]. The majority of the evaluation methods of the roughness are based on the two-dimensional fracture profiles or simple parameters that obtain a specific feature of the fracture surfaces. There is a need for new parameters to analyze the roughness.

For the influence of the roughness on the fracture, in addition to Forchheimer's law, the Izbash's law was also proposed to fit the nonlinear relationship between the flow rate and the pressure gradient [27, 28]. In the study of fracture water and sand flow, it was found that the flow performance was related to the fluid and the shape of fracture. However, they need to be analyzed in detail. The influence of roughness, concentration, particle size and aperture needs to be analyzed on the fracture seepage. Liu [29] compared the sand concentration and the influence of the sand grain flow on the water and sand fracture flow, and found that in a certain range, the concentration was the main factor. As the concentration of the fracturing agent was increased, the fracturing performance became better [30, 31]. For liquids containing particles, the permeability was found to be decreased as the concentration increased [32, 33]. Ma [34] divided the overall permeability evolution during the tests into four different phases. Particle migration formed several stages with the increase of the compression deformation. This problem was further analyzed by [35, 36]. Wang [37] and Liu [38] discussed the influence of particle size on the permeability, where water conductivity increased in along with the particle size and concentration. Li [39] and Sui [40] discussed another perspective of the problem, in which the characteristic of the water and sand migration was based on the starting pressure gradient.

The effect of the roughness of water and sand and other factors on fracture flow has also been not studied extensively. Literature shows that the influence of openness is undoubtedly the first, but the influence of roughness, concentration and particle size on the flow is not clear. Roughness plays a crucial role in the fracture seepage, while the research on water-sand flow is only based on the starting pressure gradient, and the influence of roughness and other three factors on flow has not been considered.

During the water and sand inrush in fracture, the influence of the roughness, aperture, concentration, particle size on the fracture plays a vital role considering the safety of the coal mine, but the influence of each on the flow characteristic should be further analyzed. The permeability of water and sand mixture through the fracture was tested in the study. The structure of this paper is as follows. First, the seepage tests of water and sand in fracture are explained in section 2. Then, the self-designed seepage system has been presented, which measures the permeability characteristics of the water and sand mixture in the fracture. A non-Darcy equation (approach) and the relationship between the permeability and variable *JRC* are proposed in Section 3. Experimental study on the water and sand mixture seepage in the fracture, and the results of the testing data are given. Finally, Section 5 concludes the implication of these findings. After testing the character of water and sand mixture, the model of water and sand flow is obtained. The equilibrium state of the system is

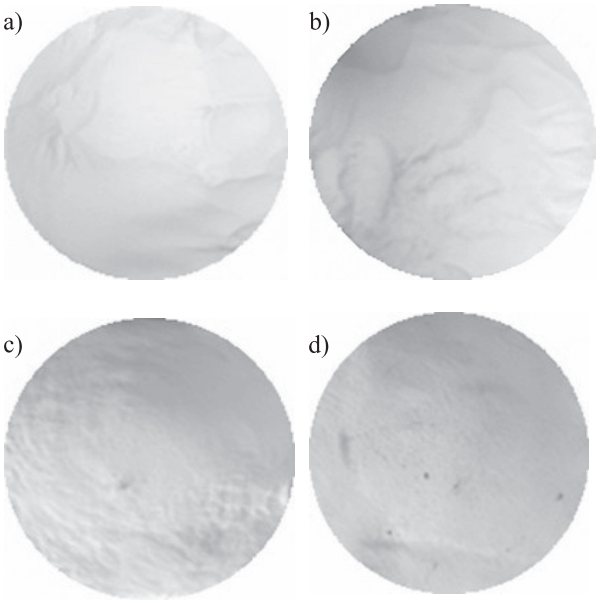

Fig. 2. Sand with different particle size: a) 0.038~0.044 mm, b) 0.061~0.080 mm, c) 0.090~0.109 mm, d) 0.120~0.180 mm.

analyzed by the little disturbed pressure and velocity respectively. This study is a good supplement to understanding the mechanism of water and sand inrush.

Seepage Tests of Water and Sand in Fracture

Characteristics of Water and Sand

The fine particle size of the mixture with water and sand were respectively, 0.038~0.044 mm, 0.061~0.080 mm, 0.090~0.109 mm and 0.120~0.180 mm, as shown in Fig. 2. The concentration of elements in water were 0.018 mol/L Ca^{2+}, 0.0126 mol/L Mg^{2+} at PH 7.0.

Experimental System

Based on the test principle, the set of experimental system was designed and fabricated as shown in Fig. 3. Water and sand were mixed in agitator (2), pressurized by sewage pump (6). conveyed to the seepage instrument (7) and collected in the water tank. During the test, the pressure and flow was gathered by the pressure transmitter (4) and flow sensor (5), respectively.

The rock employed was the sandstone from Haizi mine under 285.3 m at Anhui province, and the roughness of rock fracture was *JRC* 4~6. Sand was procured from the surface of the mine in the Northwest China. Fig.3 presents the model of the seepage in the fracture, and shows the water and sand flows through the small holes in the middle of the bottom and diffuses around the middle of the rock. According to the momentum equation, we use the formula of non-Darcy law for porous media.

$$\frac{1}{I_e}V^n + m\beta V^2 = -\frac{dp}{dr} \tag{1}$$

where $I_e = k_e/\mu_e$, the pressure is p, effective viscosity is μ_e, and effective permeability is k_e, n is power exponent. β is non-Darcy factor, V is velocity of water, r is the radius of rock sample.

The test steps are as follows:

(1) The test system was assembled according to Fig. 3, and the sample was loaded. The leakage of the experiment system was tested.

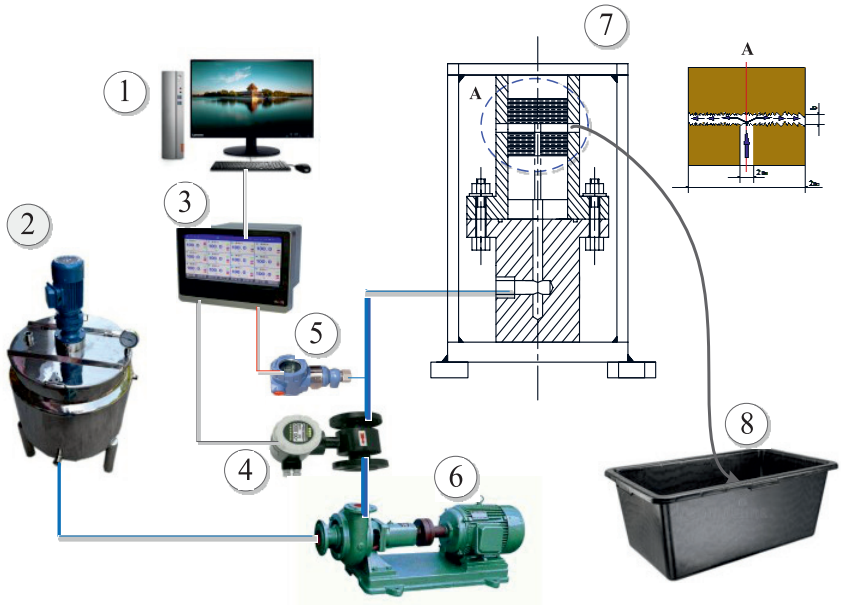

Fig. 3. Scheme of the system principles. 1. Computer; 2.Agitator; 3. Acquisition card; 4. Pressure transmitter; 5. Flow sensor; 6. Sewage pump; 7. Seepage instrument; 8. Water tank.

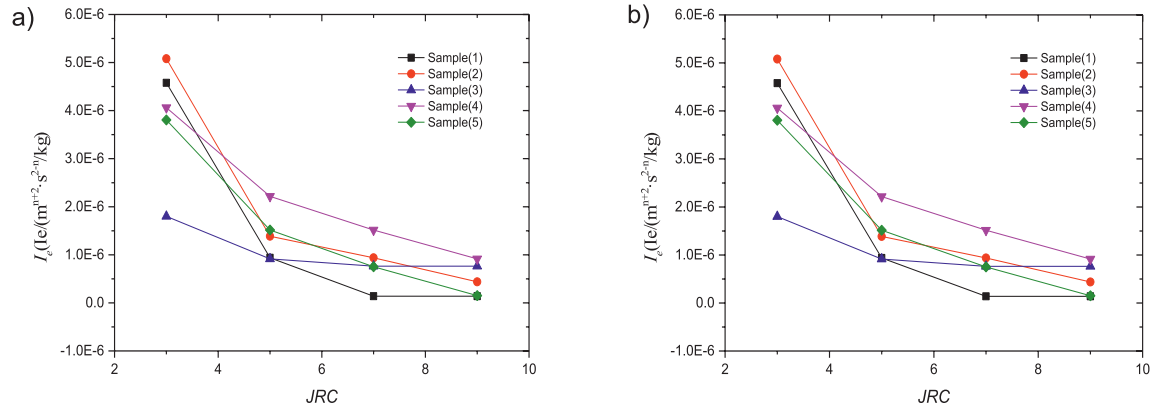

Fig. 4. Curves of permeability parameters changing with *JRC* at d_s = 0.061~0.080 mm: a) I_e-*JRC* curve under ρ_s = 20 kg/m^3, b)I_e-*JRC* curve under ρ_s = 40 kg/m^3

(2) The sand grain diameter of 0.038~0.044 mm was subjected into the mixing pool, and it was made sure that the initial concentration was from 20 kg/m^3 to 80 kg/m^3. In order to facilitate the subsequent analysis, the intermediate value was brought in the scope of the grain size.

To control the motor speed, record flow and pressure under a different rotational speed, the aperture of the fracture was set at 0.75 mm. The motor speed was changed at 200 r/min, 400 r/min, 600 r/min, 800 r/min and 1000 r/min separately. Different pressure and seepage velocities of fracture were obtained from paperless recorder, concentration of water and sand 40 kg/m^3 and 60 kg/m^3, respectively.

(3) In order to calculate conveniently, the grain diameter was changed to 0.061~0.080 mm, 0.090~0.109 mm and 0.120~0.180 mm, recorded as 0.071 mm, 0.100 mm and 0.150 mm, and the flow and pressure were recorded under different rotational speeds for each test.

(4) I_e and β were calculated from Eq. (1).

Result and Discussion

Influence of the Roughness on Permeability Parameters (Effective Fluidity)

We firstly set the width of fracture to 0.75 mm, particle size d_s=0.061~0.080 mm, and the mass concentration to 20 kg/m^3, 40 kg/m^3, 60 kg/m^3 and 80 kg/m^3, respectively; then changed the roughness. The effective fluidity along with the roughness, is shown in Fig. 4. The rock samples are processed into fractured surfaces with different roughness. Four curves of *JRC* 2-4, 4-6, 6-8, 8-10 are selected according to Barton curve, and the intermediate values of *JRC* 3,5,7,9 are directly taken as the calculation method

It was found that the relationship between the effective fluidity I_e and the roughness of the fracture belonged to the following formulas. The different fitting equations under different roughness were obtained as shown in Table 1.

Table 1. Fitted equations of permeability parameters changing with the roughness at ds = 0.061~0.080 mm.

ρ_s (kg/m^3)	Permeability para meters	Fitting equations	Correlation coefficient
20	I_e	$I_e = 6.40\times10^{-5}e^{-0.38JRC}$	0.9979
	β	$\beta = 8.10\times10^{4}e^{0.45JRC}$	0.9943
40	I_e	$I_e = 8.08\times10^{-6}e^{-0.35JRC}$	0.9246
	β	$\beta = 2.41\times10^{6}e^{0.32JRC}$	0.9946
60	I_e	$I_e = 3.75\times10^{-6}e^{-0.38JRC}$	0.9935
	β	$\beta = 1.55\times10^{6}e^{0.47JRC}$	0.9763
80	I_e	$I_e = 5.36\times10^{-6}e^{-0.44JRC}$	0.9004
	β	$\beta = 2.15\times10^{6}e^{0.43JRC}$	0.9763

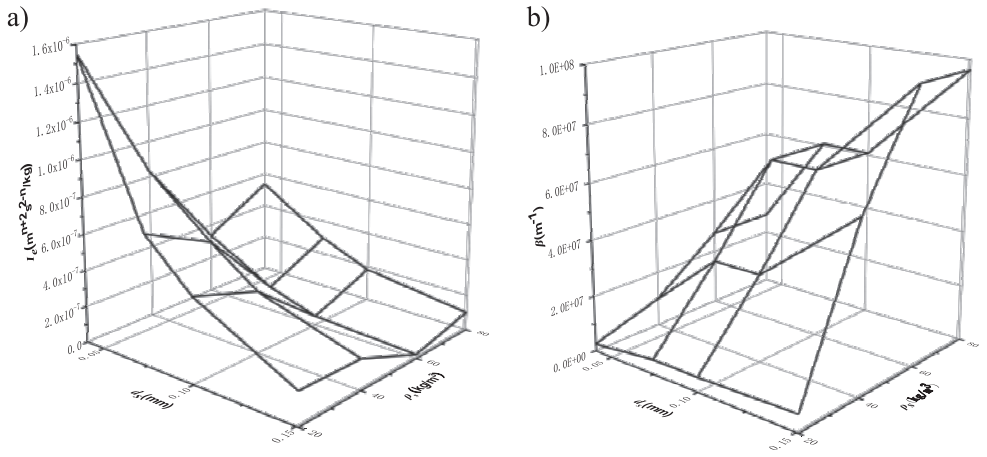

Fig. 5. Permeability parameters changing with the mass concentration and *JRC*: a) Effective fluidity, b) Non-Darcy factor.

From Fig. 4 and Table 1, it can be concluded that: under the same sand particle size and mass concentration, the effective fluidity increased monotonously with the roughness, and the effective fluidity and roughness exhibited a power exponential relationship. The non-Darcy flow factor decreased with an increase in the roughness, and the non-Darcy flow factor and roughness exhibited a power exponential relationship.

With an increase in the fracture roughness and sand mass concentration, the correlation between the permeability parameters and the fitting relation of *JRC* decreased. It is known that the roughness exhibits a significant influence on the permeability. From Cublic law, many scholars discussed the relationship between roughness and permeability. Chen [41] and Yu [42] discussed the relationship between *JRC* and permeability, and the fitting formulas were obtained.

The roughness has a great influence on the flow of water and sand fractures, and the problem of dominant path was encountered during the experiment. When the concentration was increased, the correlation decreased, which indicates that the uncertainty increases with an increase in the concentration. Fracture roughness has a significant influence on the flow of water and sand.

Keep the fracture aperture 0.75 mm, the permeability parameters are obtained by changing four particle sizes: 0.038~0.044 mm, 0.061~0.080 mm, 0.090~0.109 mm and 0.120~0.180 mm, the concentration of sand is: 20 kg/m^3, 40 kg/m^3, 60 kg/m^3, 80 kg/m^3, as shown in Fig. 5.

For the influence of effective fluidity I_e and non-Darcy factor β, sand mass concentration is the main factor, while particle size is the secondary factor. This is similar to the fact that the content of solid in soil, building materials or other solid-liquid mixtures may cause the strength of the mixture and other properties, while the particle size has a relatively small influence on it within a certain range.

The water inrush accompanied by sand inrush happened in Zhaoxian mine, which flow can attain 280 m^3/h^3 [43]. At the accident site, only flow data can be obtained, and other related concentration, roughness and other factors affecting flow are difficult to test.

Factors Influencing the Permeability

In order to obtain a better permeability of water and sand in fracture, variance analysis was used. Through comprehensive analysis, it was found that the influencing factors were fracture aperture, roughness, concentration and particle size, etc. The best seepage effect was obtained using the orthogonal transformation of four factors and four levels.

Direct Analysis

In terms of the influence of the different factors, the aperture degree was the first, followed by the roughness. In addition, the influence of concentration was higher in the experiment, but beyond a certain range, further research work is needed. As for the influencing factors of water and sand flow in fracture, the order of influence is as follows: Fracture>Roughness>Concentration>Parti cle size in the field of the test.

Fitting formulas:

Least squares regression method was used to analyze the experimental data and obtained the fitting parameters in fitting equations under the two influencing factors of particle size and concentration, and the fitting formulas of effective fluidity and non-Darcy factor were obtained in Eq. (2) and Eq. (3), and the correlation coefficients are all greater than 0.94.

$$I_e = 3.9114 d_s^{0.9795} \rho_s^{9.7697E-9} \quad (2)$$

$$\beta = 6.1970 d_s^{0.2064} \rho_s^{2.585} \quad (3)$$

In Fig. 6, the fitting data are close to the experimental data, and the error is very small.

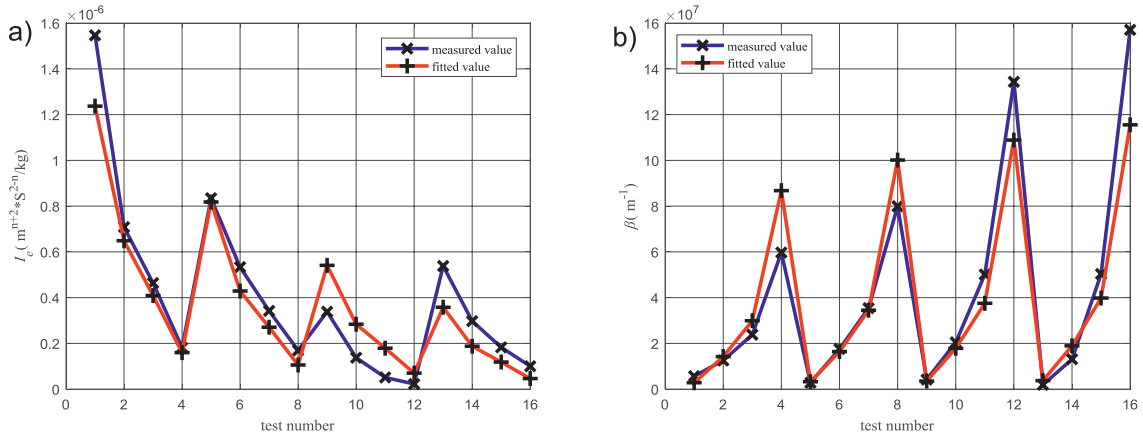

Fig. 6. Experimental data and fitting data: a) Effective fluidity, b) non-Darcy factor.

Simulation of Water and Sand Seepage in the Fracture

Fig. 7(a,b) shows the seepage velocity evolution along with the fracture length x and two kinds of sand concentration (ρ_s = 40 kg/m^3, ρ_s = 80 kg/m^3). Steady state value of seepage velocity appears at 23 s for both cases, the seepage velocity is basically synchronous along the axis. When the sand mass concentration increased from 20 kg/m^3 to 80 kg/m^3, the steady state value of the seepage velocity decreased from 1.3×10^{-2} (m/s) to 0.6×10^{-2} (m/s). In other words, the sand concentration had much influence on the seepage velocity. Fig. 7c) is the time when seepage velocity reaches steady state, *JRC* 9 needs the longest time to reach equilibrium. Velocity changes from 1.62 m/s to 0.83m/s with *JCR* 3 to 9. The steady value of seepage velocity decreases by about 40%, when *JRC* increases from 3 to 9.

The particle convey is affected by the pressure gradient, particle increase, and pressure gradient. As concentration increases, and pressure grows accordingly [44, 45]. During the flow, aperture is a visually important factor in the fluid, also the distribution of particle has an important role [46, 47].

Earlier studies considered the roughness, depth, stress, and seldom analyzed the concentration, particle size, roughness, and aperture together. Through the simulation, the result of velocity was almost same proportion to the test. In the four factors, aperture was found to be the main factor. Eq. (3) was obtained by less than 8% concentration, with an aperture less than 1mm. In fact, water and sand inrush always happened during the big fracture aperture and high concentration of sand. The roughness has a similar change trend to the average pressure drop at the adjacent points of the rock mass fracture along the seepage direction and the fluctuation of the fracture surface along the flow. The average pressure drop increases at the convex position of the wall surface, but decreases at the concave position [48]. Wang [49] introduced Pelect number to solve the dominant path problem of seepage channel. During the seepage, the stress and other factors will influence the permeability parameters [50, 51].

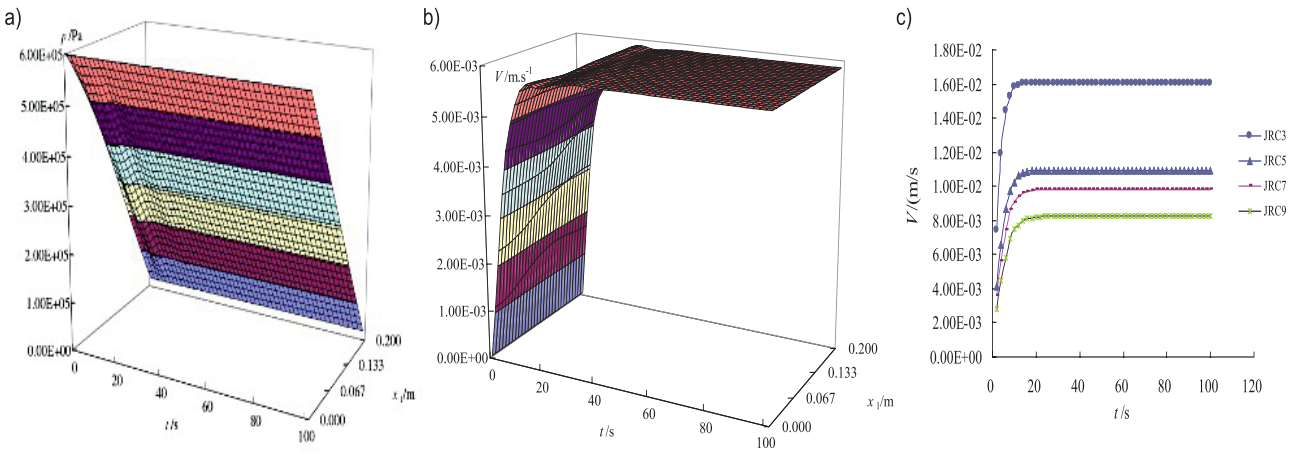

Fig. 7. Velocity time series under different roughness: a) Pressure changes at *JRC* = 3, b) Pressure changes at *JRC* = 7, c) Velocity changes.

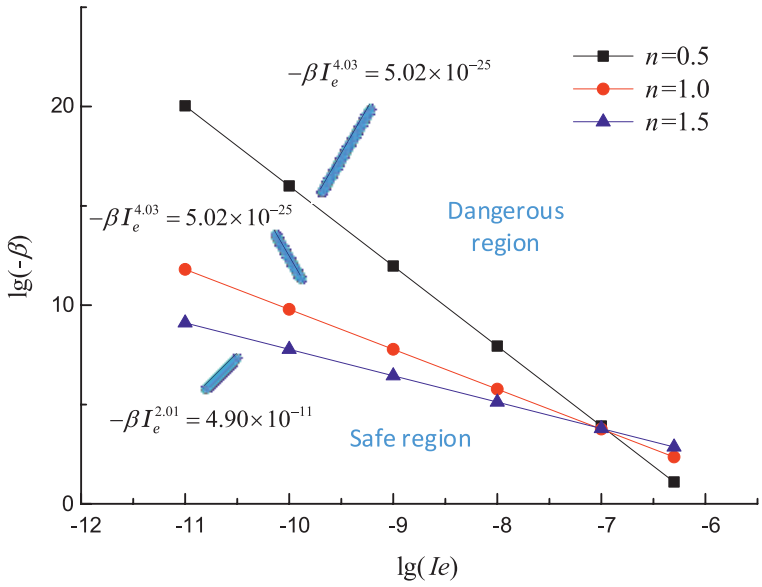

Fig. 8. Stability region of seepage system for different exponent n values (logarithmic scale).

For water and sand flow in the fracture, we can think it as the seepage system. Its equilibrium Eq. (4) comes out of Eq. (1).

$$\frac{1}{I_e}V_{st}^n + m_{p_0}\beta V_{st}^2 - \frac{p_2 - p_1}{L} = 0 \tag{4}$$

where the pressure of equilibrium state is p_{st}, seepage velocity is $V_{st,}$ and the quality is m_{st}.

The small disturbance is given by varying pressure and seepage velocity to test the system's stability zone. As shown in Fig. 8, the stability of the water and sand flow in the fracture was obtained.

Zhang [52] discussed the stability of karst collapse pillar(KCP),the seepage process in the KCP structure is a combination of pore flow, fracture flow, and pipe flow, and the transition of the seepage state is closely related to the change in the magnitude of β. Yang [53] thought that water inrush of collapse column is a dynamic process of fluid seepage from gradual change to abrupt change. The Forchheimer flow in the water inrush channel has a qualitative change from viscous resistance to viscous resistance and inertia resistance. Liu [54] gave the critical Ronald number of flow-state transformation.

Summary and Conclusions

By observing and analyzing the experimental phenomena of water and sand seepage in the fracture, it can be concluded that:

(1) The relation of the pore pressure gradient and flow velocity can be fitted by the quadratic Forchheimer equation, i.e., the water and sand flow in fracture belongs to non-Darcy flow.

(2) We designed the seepage system to test the permeability of water and sand in the fractured rock. According to the seepage test, the magnitude of the effective fluidity was in 10-8~10-5m^{n+2}. S^{2-n}/kg, while the coefficient β ranged from 10^5 to 10^8 m^{-1}.

(3) The main and secondary factors that affect the permeability include the fracture aperture, roughness, concentration and particle size.

(4) Through simulation, it was found that the roughness exhibited no significant effect on the pressure field; however, it did have a significant effect on the velocity field.

(5) The pressure distribution basically reflects the linear distribution characteristics. The disturbed value on pressure p has a greater influence on the phase trajectory.

Acknowledgments

Yu Liu wrote the manuscript, Wei Li reviewed and edited; Shuncai Li had read and agreed to the published version of the manuscript. This work was supported by the Research Fund of The State Key Laboratory of Coal Resources and safe Mining, CUMT [SKLCRSM18KF009, SKLCRSM19KF013], and the National Natural Science Foundation of China (52034007).

Conflict of Interest

The authors declare no conflict of interest.

References

1. ZHANG Y., CHAI J.R. Effect of surface morphology on fluid flow in rough fractures: A review. Journal of Natural Gas Science and Engineering, **79**, 103343, **2020**.
2. FAN L.M., MA X., JIANG H., CHEN S. Risk evaluation on water and sand inrush in ecologically fragile coal mine. Journal of China Coal Society, **41** (3), 531, **2016**.
3. ANSARIFAR M.M., SALARIJAZI M., GHORBANI K., KABOLI A.R. Spatial estimation of aquifer's hydraulic parameters by a combination of borehole data and inverse solution. Bulletin of Engineering Geology and the Environment, **79** (2), 729, **2020**.
4. ANSARIFAR M.M., SALARIJAZI M., GHORBANI K., KABOLI A.R. Simulation of groundwater level in a coastal aquifer. Marine Georsources and Geothchnology, **38** (3), 257, **2019**.
5. MA L., XU Y., NGO I., WANG Y., ZHAI J., HOU L. Prediction of Water-Blocking Capability of Water-Seepage-Resistance Strata Based on AHP-Fuzzy Comprehensive Evaluation Method – A Case Study. Water, **14**, 2517, **2022**.
6. MOFAKHAM A.A., STADELMAN M., AHMADI G. Computational modeling of hydraulic properties of a sheared single rock fracture.Transport in Porous Media, **124** (2), 1, **2018**.
7. LOUIS C. Rock hydraulic in rock mechanics.Wien, 94, **1974**.
8. NEUZIL C.E., TRACY J.V. Flow through fractures.Water Resources Research, **17** (1), 191, **1981**.
9. BARTON N., BANDIS S., BAKHTAR K.S. Deformation and conductivity coupling of rock joints. International Journal of Rock Mechanics and Mining Sciences. **22** (3), 121, **1985**.
10. QIAN X., XIA C.C., GUI Y. Quantitative estimates of non-Darcy groundwater flow properties and normalized hydraulic aperture through discrete open rough-walled joints. Internal Journal of Geomechanics. **18** (9), 04018099, **2018**.
11. AMADEI B., ILLANGASKARE T.A. Mathematical model for flow and solute transport in non-homogeneous rock fracture. International Journal of Rock Mechanics and Mining Sciences, **31** (6), 719, **1994**.
12. XIAO J., ZHU D., HILL A.D. Effects of Heterogeneity in Mineralogy Distribution on Acid-Fracturing Efficiency. Spe Production & Operations, **35** (1), 147, **2020**.
13. WANG C., JIANG Y.J., LIU J.K. Visualized experimental investigation on the hydraulic characteristics of two-phase flow in a single smooth and single rough rock fractures. Geosciences Journal, **25** (3), 351, **2021**.
14. YAO C., SHAO Y.L., YANG J.H. Effects of fracture density, roughness, and percolation of fracture network on heat-flow coupling in hot rock masses with embedded three-dimensional fracture network. Geothermics, **87**, 101846, **2020**.
15. VOGLER D., AMANN F., BAYER P., ELSWORTH D. Permeability evolution in natural fractures subject to cyclic loading and gouge formation. Rock Mechanics and Rock Engineering, **49** (9), 3463, **2016**.
16. XIE L.Z., GAO C., REN L., LI C.B. Numerical investigation of geometrical and hydraulic properties in a single rock fracture during shear displacement with the Navier-Stokes equations. Environmental Earth Sciences, **73** (11), 7061, **2015**.
17. ZHOU H.W., XIE H. Anisotropic characterization of rock fracture surfaces subjected to profile analysis. Physics Letters A, **325** (5-6), 55, **2004**.
18. DOU D., SLEEP B., ZHAN H., ZHOU Z., WANG J. Multiscale roughness influence on conservative solute transport in self-affine fractures. International Journal of H*eat* and *Mass* Transfer, **133**, 606, **2019**.
19. ISRM. International society for rock mechanics commission on standardization of laboratory and field test. International Journal of Rock Mechanics and Mining Sciences & Geomechanics Abstracts, **15** (6), 319, **1978**.
20. WANG C., WANG L., KARAKUS M. A new spectral analysis method for determining the joint roughness coefficient of rock joints. International Journal of Rock Mechanics and Mining Sciences, **113**, 72, **2019**.
21. CHEN Y., LIANG W., LIAN H., YANG J., VINH P.N. Experimental study on the effect of fracture geometric characteristics on the permeability in deformable rough-walled fractures. International Journal of Rock Mechanics and Mining Sciences, **98**, 121, **2017**.
22. BARTON N., CHOUBEY V. The shear strength of rock joints in theory and practice. Rock mechanics, **10** (12) 1, **1977**.
23. TATONE B.S.A., GRASSELLI G. A method to evaluate the three-dimensional roughness of fracture surfaces in brittle geomaterials. Review of Scientific Instrument, **80** (12), **2009**.
24. GE Y., KULATILAKE P.H.S.W., TANG H., XIONG C. Investigation of natural rock joint roughness. Computer and Geotechnics, **55**, 290, **2014**.
25. DEVELI K., BABADAGLI T. Experimental and visual analysis of single-phase flow through rough fracture replicas. International Journal of Rock Mechanics and Mining Sciences, **73**, 139, **2015**.
26. LI Y., HUANG R. Relationship between joint roughness coefficient and fractal dimension of rock fracture surfaces. International Journal of Rock Mechanics and Mining Sciences, **75**, 15, **2015**.
27. RONG G., HOU D., YANG J., CHENG L., ZHOU C.B. Experimental study of flow characteristics in non-mated rock fractures considering 3D definition of fracture surfaces. Engineering Geology, **220**, 152, **2017**.
28. CHEN Y.D., LIAN H.J., LIANG W.G., YANG J.F., NGUYEN V.P., BORDAS S.P.A. The influence of fracture geometry variation on non-Darcy flow in fractures under confining stresses. International Journal of Rock Mechanics and Mining Sciences, **113**, 59, **2019**.
29. ZHAO Y.L., ZHANG Y.L., WANG W.J., TANG J.Z., LIN.H., WAN W. Transient pulse test and morphological analysis of single rock fractures. International Journal of Rock Mechanics and Mining Sciences, **91**, 139, **2017**.
30. ROOSTAEI M., NOURI A., FATTAHPOUR V. Coupled Hydraulic Fracture and Proppant Transport Simulation. Energies, **13** (11), 2822, **2020**.
31. FAN M., MCCLURE J., HAN Y.H. Using an Experiment/Simulation-Integrated Approach To Investigate Fracture-Conductivity Evolution and Non-Darcy Flow in a Proppant-Supported Hydraulic Fracture. SPE Journal, **24** (4), 1912, **2019**.
32. ANBAR S., THOMPSON K.E., TYAGI M. The Impact of Compaction and Sand Migration on Permeability and Non-Darcy Coefficient from Pore-Scale Simulations. Transport in Porous Media, **127** (2), 247, **2019**.

33. YANG S.Y., RUSSELL T., BADALYAN A. Characterisation of fines migration system using laboratory pressure measurements. Journal of Natural Gas Science and Engineering, **65**, 108, **2019**.
34. MA D., MOHAMMAD R., YU H.S., BAI H.B. Variations of hydraulic properties of granular sandstones during water inrush: Effect of small particle migration. Engineering Geology. **217**, 61, **2017**.
35. WANG L.Z., KONG H.L. Variation Characteristics of Mass-Loss Rate in Dynamic Seepage System of the Broken Rocks. Geofluid, UNSP 7137601, **2018**.
36. KONG H.L., WANG L.Z. The behavior of mass migration and loss in fractured rock during seepage. Bulletin of Engineering Geology and the Environment, **79** (2), 739, **2020**.
37. WANG L.Z., KONG H.L. The Mass Loss Behavior of Fractured Rock in Seepage Process: The Development and Application of a New Seepage Experimental System. Advances in Civil Engineering, 7891914, **2018**.
38. LIU J.K., CHEN W.Z., NIE W. Experimental Research on the Mass Transfer and Flow Properties of Water Inrush in Completely Weathered Granite Under Different Particle Size Distributions. Rock Mechanics and Rock Engineering, **52** (7), 2141, **2019**.
39. LI W.P., LIU Y., QIAO W. An Improved Vulnerability Assessment Model for Floor Water Bursting from a Confined Aquifer Based on the Water Inrush Coefficient Method. Mine Water and the Environment, **37** (1), 196, **2018**.
40. LIANG Y.K., SUI W., QI J.F. Experimental investigation on chemical grouting of inclined fracture to control sand and water flow. Tunnelling and Underground Space Technology, **83**, 82, **2019**.
41. CHEN Y.F., ZHOU J.Q., HU S.H., HU R., ZHOU C.B. Evaluation of Forchheimer equation coefficients for non-Darcy flow in deformable rough-walled fractures. Journal of Hydrology, **529**, 993, **2015**.
42. YU X., REGENAUER-LIEB K., TIAN F.B. Effects of surface roughness and derivation of scaling laws on gas transport in coal using a fractal-based lattice Boltzmann method. Fuel, **259**, 116229, **2020**.
43. QIAO W., WANG Z.W., LI W.P., LU Y.G., LI L.G., HUANG Y. HE J.H., LI X.Q., ZHAO S.L., LIU M.N. Formation mechanism,disaster-causing mechanism and prevention technology of roof bed separation water disaster in coal mines. Journal of China coal society, 46 (2), 507, **2021**.
44. HUANG F.S., KANG Y.L., YOU Z.J. Critical Conditions for Massive Fines Detachment Induced by Single-Phase Flow in Coalbed Methane Reservoirs: Modeling and Experiments. Energy&Fuels, **31** (7), 6782, **2017**.
45. YANG X.Y., CAI J.H., JIANG G.S. Nanoparticle plugging prediction of shale pores: A numerical and experimental study. Energy, **208**, 118337, **2020**.
46. SONG Z.J., BAI B.J., ZHANG H. Preformed particle gel propagation and dehydration through semi-transparent fractures and their effect on water flow. PSE Journal, **167**, 549, **2018**.
47. LIU Y., HAN Y., ZHANG Q., LI M., WANG Z.F. Analysis of water and sand seepage characteristics in fracture. Journal of China Coal Mining, **44** (3), 874, **2019**.
48. SHE L.F., CENG Y., WANG Z.L., LI S.J. Research on seepage properties of rough fracture considering geometrical morphology. Chinese Journal of Rock Mechanics and Engineering, **38** (S1), 2704, **2019**.
49. WANG Z.H., ZHOU C.T., WANG F., LI C.B., XIE H.P. Channeling flow and anomalous transport due to the complex void structure of rock fractures. Journal of Hydrology, **601**, 126624, **2021**.
50. NIE Y.N., ZHANG G.Q., WEN J., LI S.Y., ZHOU D.W. Cyclic injection to reduce hydraulic fracture surface roughness in glutenite reservoirs. International Journal of Rock Mechanics and Mining Sciences, **142**, 104740, **2021**.
51. TEKLU T.W., ABASS H.H., HANASHMOONI R., CARRATU J.C. Experimental investigation of acid imbibition on matrix and fractured carbonate rich shales. Journal of Natural Gas Science and Engineering, **45**, 706, **2017**.
52. ZHANG T.J., PANG M.K., ZHANG X.F., PAN H.Y. Determining the Seepage Stability of Fractured Coal Rock in the Karst Collapse Pillar. Advances in Civil Engineering, 1909564, **2020**.
53. YANG T.H., SHI W.H., LIU H.L., YANG B., YIN X., LIU Z.B. A non-linear flow model based on flow translation and its application in the mechanism analysis of water inrush through collapse pillar. Journal of China Coal Socity, **42** (2), 315, **2017**.
54. LIU L.H., WU X.X. Research of transition between the Darcican and non-Darcican flow of rock block scale. Bulletin of Science and Technology, **33** (1), 32, **2017**.